

Photoinduced electron transfer across a gold supported octadecanethiol/phosphatidylcholine hybrid bilayer membrane mediated by C₆₀ in different redox species solution

Dianlu Jiang^{a,*}, Junxin Li^a, Peng Diao^a, Zhenbin Jia^a, Ruting Tong^a,
H. Ti Tien^b, Angelica L. Ottova^b

^a Department of Chemistry, Hebei Teacher's University, Shijiazhuang 050016, China

^b Membrane Biophysics Laboratory (Giltner Hall), Department of Physiology, Michigan State University, East Lansing, MI 48824, USA

Received 14 May 1999; received in revised form 8 November 1999; accepted 20 November 1999

Abstract

Electron transfer across the biomembrane is central to photosynthesis, to mitochondrial respiration and to the design of molecular systems for solar energy conversion. We report here that gold supported octadecanethiol/phosphatidylcholine hybrid bilayer membrane mediated by C₆₀ (abbreviated C₆₀ HBM) can act as both a photosensitizer for electron transfer from a donor molecule and a mediator for electron transport across a hybrid bilayer membrane. The steady-state photocurrent behaviors in different concentration of ascorbate, Co(bpy)₃^{2+/3+} or Fe(CN)₆^{4-/3-} solution have been studied. The rate-limiting step of the whole photoinduced electron transfer depends on the applied potential and the redox concentration in solution. The C₆₀ HBM electrode was fabricated for the first time and there is no investigation on C₆₀ incorporated octadecanethiol/phosphatidylcholine hybrid bilayer membrane in literature. The sigmoidal-shaped steady-state photocurrent versus the applied potential curve is first observed and it is different from the linear-shaped i_{ph}/E curve of C₆₀ modified bilayer lipid membrane reported by Bensasson et al. [R.V. Bensasson, J.-L. Garaud, S. Leach, G. Miquel, P. Seta, Chem. Phys. Lett. 210 (1993) 141]. © 2000 Elsevier Science S.A. All rights reserved.

Keywords: C₆₀; Photosensitizer; Electron transfer; Hybrid bilayer

1. Introduction

The electron transfer across the lipid membrane is a fundamental property of living systems and is exemplified in photosynthesis. The design of molecular systems for solar energy conversion mimics this vectorial photoinduced charge transportation [1–4]. Fullerenes, due to their unique structure and good photosensitizing and electron transfer properties, have been incorporated in the bilayer lipid membrane (BLM) for investigation of photoinduced electron transfer across the BLM [1–3,5–8]. Hwang et al. measured the charge transit time across the BLM containing fullerenes (C₆₀ and C₇₀) and believed that the conduction was electronic [8], also they investigated the factors of light, donor, acceptor, and C₇₀ concentration on the magnitude of photocurrent, found out that the light intensity and donor concentration were the limiting factors. The

photocurrent increased quickly and reached a plateau at ~0.7 mM C₇₀, probably because of limited C₇₀ solubility in the BLM [3]. But Niu et al. [2] believed that the C₇₀ molecules in the BLM formed aggregates with small aggregation number when C₇₀ concentration was high enough, which was verified by the similarity of the absorption spectrum of C₇₀ in ethyl acetate-water (1% water) mixture and the action spectrum of the steady state photocurrent of the dithionate|C₇₀|ferricyanide system. C₇₀ aggregates could rapidly and efficiently transport charge across the bilayer system. The results of Bensasson et al. supported those of Niu et al. Bensasson et al. [5] found that the i_{ph}/E (the steady-state photocurrent versus the applied potential) curve was almost linear from –150 to 100 mV. This is consistent with an electron-hopping mechanism and they believed that the electron transfer from the fullerene anion at the reduction interface occurred through fullerene aggregates in which the charge were transferred by electron hopping and ultimately reach the oxidizing entities at the opposite interface. Each fullerene molecule taking part in this electron transfer

* Corresponding author.

E-mail address: dianlu@sj-user.he.cninfo.net (D. Jiang)

process exists firstly in anionic and then in neutral ground state. Tien et al. [6,7] used the solid supported bilayer lipid membrane (s-BLM) containing C_{60} as sensors for detecting I^- , the sensitivity of the C_{60} -containing s-BLM to I^- was excellent with a linear response in the range from 10^{-8} to 10^{-2} M.

However, the small range of applied voltage and the fragility of the BLM limit both its applications for developing devices of practical use and the possibility of the intensive study during its lifetime. Moreover, with the planar BLM (p-BLM), in the case of electron transfer, it is too complicated, because at least two BLM/solution interfaces are involved. But with the metal supported BLM, due to the low work function of metal, the influence of the metal/BLM interface on the whole electron transfer processes can be neglected. Furthermore, in contrast to the case of the p-BLM, because of the blocking effect of the substrate to the ion transportation, the ion translocation effect can be ruled out. Consequently for the metal supported BLM, the whole electron transfer processes are simplified. The s-BLM has a good stability, but it often has distinct defects (such as pinholes), therefore the electron transfer at these defects often interfere with or even cover up transmembrane electron transfer. Thus, it is not a good model for the study of transmembrane electron transfer. Herein, we adopt the method of Ding et al. [9] using a self-assembled octadecanethiol monolayer on gold as a phosphatidylcholine support to fabricate the hybrid bilayer membrane (HBM) and report the photovoltage and photocurrent measurements on this new system. The experimental results suggest that upon illumination, C_{60} molecules absorb photons and become $^3C_{60}$, under the intrinsic electric field or applied electric field, and in the presence of electron donors in solution, electrons transfer via C_{60} small aggregates vectorially [2,5] across the HBM. The rate of whole transmembrane process is dependent on the applied potential and the donor concentration in solution.

Also our experimental results show that this kind of HBM has no distinct defects (pinholes) and has good stability, so it is a better model than the p-BLM and the s-BLM in studying the transmembrane electron transfer mechanism.

2. Experimental

2.1. Materials

Octadecanethiol (Aldrich) was a generous gift from Mr. Zhongfan Liu (Beijing University), used as received. The lipid solution was prepared by dissolving 25 mg C_{60} in 2 ml toluene and then added this solution to 20 ml 2% phosphatidylcholine in squalene. $Co(bpy)_3(ClO_4)_3 \cdot 3H_2O$ (Tris-2,2'-bipyridyl cobalt(III) perchlorate trihydrate) and $Co(bpy)_3(ClO_4)_2$ (Tris-2,2'-bipyridyl cobalt(II) perchlorate) were synthesized and purified according to the literature

[10] and they were verified by the UV–VIS spectroscopy according to the literature [11]. All other chemicals are of reagent grade and used without further purification. Aqueous solutions are prepared with deionized-distilled water.

2.2. Apparatus and methods

2.2.1. Apparatus

Cyclic voltammetry and electrochemical impedance spectroscopy were performed with an electrochemical system (EG&G PARC) which includes a Model 273 potentiostat/galvanostat and a Model 5208 two-phase lock-in analyzer and a 486 personal computer.

The open circuit photovoltage of the C_{60} HBM in solution was measured by a Stanford Research Model 510 lock-in amplifier. For photocurrent measurements, the potential applied to the C_{60} HBM is performed with an EG&G PARC Model 363 potentiostat/galvanostat and the steady state photocurrent was measured by a Stanford Research Model 510 lock-in amplifier. The output of the Shimadzu tungsten light source was monochromated by a 1350 grooves/mm grating monochromator and was chopped by using a Stanford Research Model 540 chopper controller.

2.2.2. Methods

All electrochemical experiments were carried out in a conventional three-electrode system. The saturated calomel electrode (abbreviated SCE) was used as a reference electrode and a large area Pt electrode as a counter electrode. All potentials reported here are referred to SCE. All experiments were carried out at room temperature.

The gold supported octadecanethiol self-assembled monolayer electrode was prepared according to the literature [12]. In our experiments, in order to avoid uncertainties in photoelectrochemical responses, the gold supported octadecanethiol self-assembled monolayer electrode must be structurally well-ordered and relatively defect-free (that means no pinholes). The self-assembled octadecanethiol monolayer electrodes were checked by AC impedance spectroscopy and cyclic voltammetry. Electrodes, which have pinholes, were not used.

After the electrochemical check-up, the Au electrode coated with thiol monolayer was immersed in deionized-distilled water for about 2 h and washed with deionized-distilled water and dried with a stream of nitrogen. Immediately, some lipid (containing C_{60}) solution was put on the surface of the octadecanethiol modified gold electrode and transferred into a bathing solution of 0.1 mol l^{-1} KCl at once. After about 12 h spontaneous thinning, the electrodes were monitored by AC impedance spectroscopy and by cyclic voltammetry. When the capacitance [9] approached $0.5 \mu \text{ F cm}^{-2}$, the bilayer was assumed as satisfactory and then a series of photoelectrochemical measurements were carried out.

3. Results and discussion

3.1. Open circuit photovoltage spectrum

We use the open circuit photovoltage of 2CR1227-01 silicon photovoltaic cell (2CR1227-01 silicon photovoltaic cell, Beijing photoelectronic devices factory) to determine the light quantum distribution of light source and the open circuit photovoltage of the C₆₀ HBM electrode under the same condition to determine the light quantum efficiency (normalized) as shown in Fig. 1.

From the curve in Fig. 1, we can see the broad photovoltage spectrum with a peak around 600 nm. This spectrum is similar to the absorption spectrum of C₆₀ in *n*-hexane solution [13]. It is quite different from the photovoltage spectrum of polycrystalline film of C₆₀ [14]. This indicates that the C₆₀ in the BLM exists in dissolved form or small aggregates rather than C₆₀ crystal or large aggregates [2]. Another point needed to be addressed is the existence of photovoltage which is indicative of charge separation across the BLM, an explanation is that upon illumination the ³C₆₀ is formed, at the membrane/solution interface, the donor (impurities or water, the standard redox potential of water, E_{O₂/H₂O}⁰, at pH=7, is 0.5631 V vs. SCE, which is much more smaller than E_{⁰_{3C₆₀/C₆₀-} = 1.14 V vs. SCE, so the electron transfer between H₂O and ³C₆₀ is possible, ³C₆₀ + (1/2)H₂O → H⁺ + (1/4)O₂ + C₆₀⁻) gives electron to ³C₆₀, the electron is delocalized (Rao et al. [15] have shown that a C₆₀ film, irradiated by visible or UV light, photopolymerizes via the possible formation of (=C=C=) bridges between adjacent fullerenes) and the intrinsic electric field is formed, thus a photovoltage across HBM is formed.}

To find the limiting factors and clarify the transmembrane electron transfer mechanism, we investigated the effect of the concentration of redox species in solution and of the applied potential on the magnitude of the steady-state photocurrent.

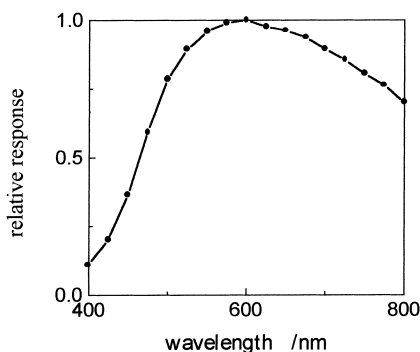


Fig. 1. Relative response of C₆₀ HBM electrode in 0.1 mol l⁻¹ KCl solution (normalized), frequency 14 Hz.

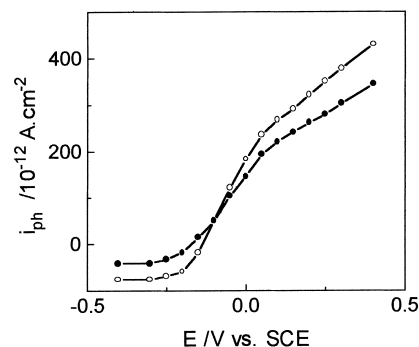


Fig. 2. Steady-state photocurrent versus applied potential in ascorbate solution (concentration [●] 39.64, [○] 80.00 mM), excitation wavelength 600 nm, frequency 14 Hz.

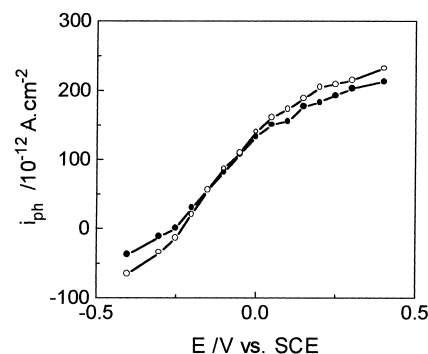


Fig. 3. Steady-state photocurrent versus applied potential in Co(bpy)₃^{2+/3+} solution (concentration [●] 0.42, [○] 0.89 mM), excitation wavelength 600 nm, frequency 14 Hz.

3.2. Photocurrent (*i_{ph}*) versus potential (*E*) characteristics

The steady state photocurrent (*i_{ph}*) in different redox species solution was measured (shown in Figs. 2–4). In all three cases, sigmoidal-shaped curves and mainly positive photocurrents are observed. The photocurrent (*i_{ph}*) varies linearly from -0.15 to 0.05 V vs. SCE, the coefficients are all higher than 0.99, and beyond this potential region the photocurrents tend to be saturated. In all three cases the observation of mainly positive photocurrent at all potentials

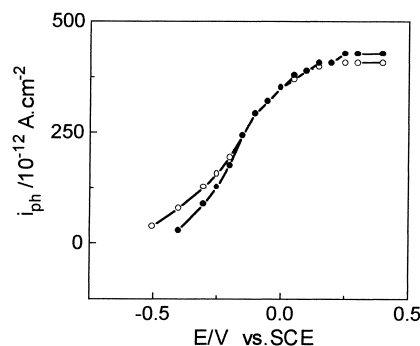


Fig. 4. Steady-state photocurrent versus applied potential in Fe(CN)₃^{4-/3-} solution (concentration [●] 2.91, [○] 1.96 mM), excitation wavelength 600 nm, frequency 14 Hz.

indicates that mainly the photoinduced oxidation of donor in solution occurs.

An i_{ph}/E non-linear characteristic has been observed in the case of tetraphenylboron anions [16] and monomeric porphyrins [17]. The non-linearity of the i_{ph}/E curve results from the non-linear dependence of the ion translocation rate on the transmembrane electric field. In our cases, as stated in the introduction section, the non-linearity of i_{ph}/E curve is unlikely caused by the fullerene ion translocation.

On the other hand, the i_{ph}/E curve should be almost linear in the case of transmembrane intramolecular/intermolecular multistep electron transfer [4,18–20]. In the present case of membranes, the linear shape of the i_{ph}/E characteristic from -0.15 to 0.05 V vs. SCE suggests that the dominant mechanism is electron hopping [18] within the bilayer medium rather than translocation of fullerene anions. Because the whole photoinduced transmembrane electron transfer process involves two processes, (1) electron transfer between donor in solution and photoinduced ${}^3C_{60}$ at the membrane/solution interface and the formation of C_{60}^- , (2) electron transfer through C_{60} small aggregates across the HBM in which the charge were transferred by electron hopping, and in which each C_{60} molecule taking part in this electron hopping process exists successively in the anionic and the neutral ground state. The sigmoidal-shaped i_{ph}/E characteristic may be an indication of change in electron transfer limiting step.

Also in all three cases at the potentials more negative than -0.15 V vs. SCE, only small photocurrents are observed. This may be a support of existence of the intrinsic electric field, which is caused by the difference in Fermi levels between the gold substrate and solution. This phenomenon is in agreement with the current response under different overpotential of an n-type semiconductor/liquid junction. As the potential goes negative the inner electric field decreases, so does the rate of charge transport in the HBM; likewise, as the applied potential goes positive, the inner electric field increases, the electron separation and migration become faster, so a linear i_{ph}/E appears. As the potential goes negative further, the electron separation and migration is blocked because almost no electron acceptor can take an electron from ${}^3C_{60}$ thermodynamically. The negative small photocurrents at far negative potential (for example, less than -0.2 V vs. SCE) might result from dissolved impurities or water. The linear dependence of photocurrent on applied potential indicates that the electron separation and migration in the HBM is the limiting step of the whole photoinduced transmembrane electron transfer. At potentials higher than 0.05 V vs. SCE, the i_{ph}/E curves change much more slowly and tend to reach plateau, an explanation is that when the potential goes positive, the inner electric field is getting higher, so is the rate of charge transport across the HBM, therefore the limiting step changes from the inner charge transport to the interfacial electron transfer between redox couple in solution and ${}^3C_{60}$ in the HBM. This also can be seen from the i_{ph}/C curves under different redox concentration (Figs. 5–7).

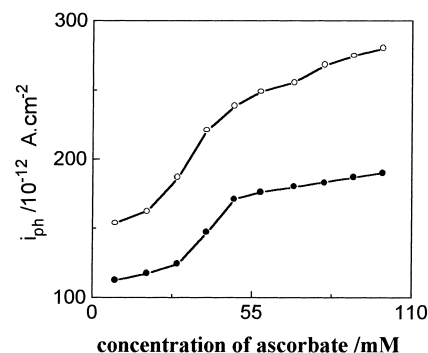


Fig. 5. Steady-state photocurrent versus ascorbate concentration (applied potential [●] 0.00, [○] 0.10 V vs. SCE), excitation wavelength 600 nm, frequency 14 Hz.

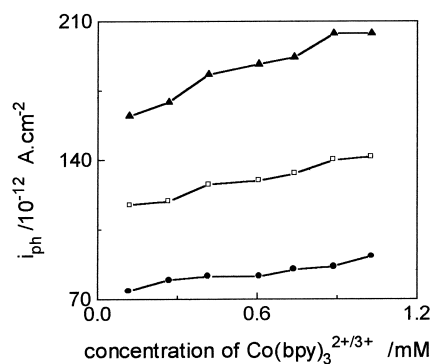


Fig. 6. Steady-state photocurrent versus $Co(bpy)_3^{2+/3+}$ concentration (applied potential [●] -0.1 , [□] 0.00, [▲] 0.2 V vs. SCE), excitation wavelength 600 nm, frequency 14 Hz.

3.3. Photocurrent (i_{ph}) variation versus concentration (C) characteristics

In order to examine the influence of the concentration of redox couple on the transmembrane electron transfer process, we changed the concentration of the redox couple in solution and measured the photocurrent of the C_{60} HBM electrode at given potential with different concentrations of redox couple, as shown in Figs. 5–7. For all three different

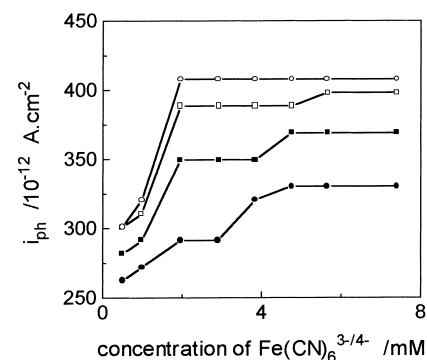


Fig. 7. Steady-state photocurrent versus $Fe(CN)_6^{4-/3-}$ concentration (applied potential [●] -0.10 , [■] 0.00, [□] 0.1, [○] 0.2 V vs. SCE), excitation wavelength 600 nm, frequency 14 Hz.

redox couples, in low concentration region the photocurrents increase monotonically with the redox species concentration. In the cases of ascorbate and $\text{Fe}(\text{CN})_6^{4-/3-}$, the photocurrents tend to reach plateaus. Also it can be seen that the more positive the applied potential is, the higher the photocurrent is. All these demonstrate that in low concentration region the dominant step of the whole photoinduced transmembrane electron transfer process is the interfacial electron transfer reaction, with the donor concentration increasing, the limiting step shifts from interfacial electron transfer to the charge transfer across HBM. Another feature that can be seen is that as the donor concentration approaches zero the photocurrent does not approach zero, which is contradictory with the above argument. An only explanation is that water (the standard redox potential of water, $E_{\text{O}_2/\text{H}_2\text{O}}^0$ at pH=7, is 0.5631 V vs. SCE) in solution can act as electron donor, this fact prevents us from getting more specific photocurrent dependence on donor concentration.

3.4. Thermodynamic considerations

Although the standard redox potentials have been measured in solvents different from ours, a fine estimation can be made for our case. The reduction potential is known for fullerenes, and we can adopt $E_{\text{C}_{60}/\text{C}_{60}^-}^0 = -0.42$ V vs. SCE [21]. The reduction potential of ${}^3\text{C}_{60}$ should be higher than that of the ground state by the amount of triplet energy, 1.56 eV [21], so that $E_{{}^3\text{C}_{60}/\text{C}_{60}^-}^0$ should be $1.56 - 0.42 = 1.14$ V vs. SCE. The redox potentials of redox couples in solution are $E_{\text{ascorbate}_{\text{ox}}/\text{ascorbate}_{\text{red}}}^0 = -0.21$ V vs. SCE [18], $E_{\text{Co}(\text{bpy})_3^{3+/2+}}^0 = 0.07$ V vs. SCE, $E_{\text{Fe}(\text{CN})_6^{3-/4-}}^0 = 0.22$ V vs. SCE. The photoreduction of fullerene triplet ${}^3\text{C}_{60}$ by redox couples in solution is thus highly exergonic with ΔG^0 being approximately -1.35 eV for ascorbate oxidation, -1.07 eV for $\text{Co}(\text{bpy})_3^{2+}$ oxidation and -0.92 eV for $\text{Fe}(\text{CN})_6^{4-}$ oxidation.

In contrast, the photooxidation of ${}^3\text{C}_{60}$ can be estimated to be endergonic. Taking $E_{\text{C}_{60}^+/\text{C}_{60}}^0 = 1.8$ V vs. SCE [18], the value of $E_{\text{C}_{60}^+/\text{C}_{60}}^0$ is $1.8 - 1.56 = 0.24$ V vs. SCE, and ΔG^0 should be 0.17 eV for $\text{Co}(\text{bpy})_3^{3+}$ reduction and 0.02 eV for $\text{Fe}(\text{CN})_6^{3-}$ reduction. As the value of $E_{\text{O}_2/\text{H}_2\text{O}}^0$ (0.5631 V vs. SCE) is higher than that of $E_{\text{C}_{60}^+/\text{C}_{60}}^0$ (0.24 V vs. SCE), the oxygen in solution can oxidize ${}^3\text{C}_{60}$ to C_{60}^+ , thermodynamically. However, the concentration of oxygen in solution is very low, as a result, the negative photocurrents due to ${}^3\text{C}_{60}$ oxidation are covered up by the positive photocurrent due to ${}^3\text{C}_{60}$ reduction. From these roughly estimated data above we can see that ${}^3\text{C}_{60}$ photoreduction is thermodynamically possible much more than ${}^3\text{C}_{60}$ oxidation, so the i_{ph}/E response is in agreement with the current response of n-type semiconductor/liquid junction under different overpotentials. These rough thermodynamic considerations indicate

that the major part of the electron transfer process may occur via the photoreduction of triplet ${}^3\text{C}_{60}$ at the membrane/solution interface.

4. Conclusion

Overall the linear shape of the i_{ph}/E characteristic from -0.15 to 0.05 V vs. SCE suggests that the dominant mechanism is electron hopping across the bilayer medium rather than translocation of fullerene anions. The photoinduced electron transfer at certain C_{60} concentration in the HBM at the given incident light intensity depends on the electric field or the across-membrane potential and donor concentration in solution. The limiting step of overall photoinduced transmembrane electron transfer, dependent on these factors, is changeable. The non-zero photocurrent of the C_{60} HBM electrode in solution without redox species is first observed here, demonstrates that water can act as electron donor for photoreduction of ${}^3\text{C}_{60}$.

The results of our study are consistent with a mechanism of photoinduced electron transport in initially or dynamically aggregated fullerenes in the phospholipid bilayer membrane. The lifetime, τ , of ${}^1\text{C}_{60}$ (1.2 ns) and that of ${}^3\text{C}_{60}$ (410 μs) [1] favor the involvement of ${}^3\text{C}_{60}$ in the electron transfer process.

Acknowledgements

The authors gratefully acknowledge the support of Science Foundation of Hebei Province and the generous gift from Mr. Zhongfan Liu (Beijing University).

References

- [1] K.C. Hwang, D. Mauzerall, Vectorial electron transfer from an interfacial photoexcited porphyrin to ground-state C_{60} and C_{70} and from ascorbate to triplet C_{60} and C_{70} in a lipid bilayer, *J. Am. Chem. Soc.* 114 (1992) 9705.
- [2] S. Niu, D. Mauzerall, Fast and efficient charge transport across a lipid bilayer is electronically mediated by C_{70} aggregates, *J. Am. Chem. Soc.* 118 (1996) 5791.
- [3] K.C. Hwang, D. Mauzerall, Photoinduced electron transport across a lipid bilayer mediated by C_{70} , *Nature* 361 (1993) 138.
- [4] A. Lamrabet, M. Momenteau, P. Mailard, P. Seta, Photoinduced electron wire properties of supramolecular stacked triporphyrins incorporated in lipid bilayers. Contribution of a leakage current under voltage polarization, *J. Molecular Electronics* 6 (1990) 145.
- [5] R.V. Bensasson, J.-L. Garaud, S. Leach, G. Miquel, P. Seta, Transmembrane electron transport mediated by photoexcited fullerenes, *Chem. Phys. Lett.* 210 (1993) 141.
- [6] H.T. Tien, L.-G. Wang, X. Wang, A.L. Ottova, Electronic-processes in supported bilayer lipid membranes (s-BLM) containing a geodesic form of carbon (fullerene C_{60}), *Bioelectrochem. Bioenerg.* 42 (1997) 161.
- [7] L.-G. Wang, X. Wang, A.L. Ottova, H.T. Tien, Iodide-sensitive sensor based on a supported bilayer lipid membrane containing a cluster form of carbon (fullerene C_{60}), *Electroanalysis* 8 (1996) 1020.

- [8] K.C. Hwang, S. Siu, D. Mauzerall, Electron transport across a lipid bilayer mediated by fullerenes, *Proc.-Electrochem. Soc.* (1994) 94-24 (Recent Advances in the Chemistry and Physics of Fullerenes and Related Materials), 845.
- [9] L. Ding, J.H. Li, S.J. Dong, Supported phospholipid membranes: comparison among different deposition methods for a phospholipid monolayers, *J. Electroanal. Chem.* 416 (1996) 105.
- [10] F.H. Burstall, R.S. Nyholm, Studies in co-ordination chemistry Part XIII, Magnetic movements and bond types of transition-metal complexes, *J. Chem. Soc.* (1952) 3570.
- [11] B. Martin, G.M. Waind, 2:2'-Dipyridyl complexes of cobalt, rhodium, and iridium Part I, Trivalent rhodium and complexes, *J. Chem. Soc.* (1958) 4284.
- [12] C.D. Bain, E.B. Troughton, Y.T. Tao, J. Evall, G.M. Whitesides, R.G. Nuzzo, Formation of monolayer films by the spontaneous assembly of organic thiols from solution onto gold, *J. Am. Chem. Soc.* 111 (1989) 321.
- [13] H. Ajie, M.M. Alvarez, S.J. Anz, R.D. Beck, F. Diederich, K. Fostiropoulos, D.R. Huffman, W. Kratschmer, Y. Rubin, K.E. Schriver, D. Sensharma, R.L. Whetten, Characterization of the soluble all-carbon molecules C₆₀ and C₇₀, *J. Phys. Chem.* 94 (1990) 8630.
- [14] B. Miller, J.M. Rosamilia, G. Dabbagh, R. Tycho, R.C. Haddon, A.J. Muller, W. Wilson, D.W. Murphy, A.F. Hebard, Photoelectrochemical behavior of C₆₀ film, *J. Am. Chem. Soc.* 113 (1991) 6291.
- [15] A.M. Rao, P. Zhou, K.A. Wang, G.T. Hager, J.M. Holden, Y. Wang, W.T. Lee, X.X. Bi, P.C. Eklund, D.S. Cornett, M.A. Duncan, I.J. Amster, Photoinduced polymerization of solid fullerene (C₆₀) films, *Science* 259 (1993) 955.
- [16] C. Gavach, R. Sandeaux, P. Seta, A potentiostatic study of hydrophobic ion transfer across lipid bilayer Part I, Case of zero ion fluxes in adsorption and desorption processes, *J. Electroanal. Chem.* 413 (1975) 33.
- [17] E. Bienvenue, P. Seta, A. Hofmanova, Steady-state photocurrents associated with electron transfer through planner bilayers sensitized by zinc 5, 10, 15, 20-tetraphenylporphyrins, *J. Electroanal. Chem.* 162 (1984) 275.
- [18] S. Licht, O. Khaselev, P.A. Ramakrishnan, D. Faiman, E.A. Katz, A. Shames, S. Goren, The photochemistry of single crystal fullerenes, *Proc. Electrochem. Soc.* (1997) 97-20 (photoelectrochemistry), 368.
- [19] P. Seta, E. Bienvenue, A.L. Moore, T.A. Moore, D. Gust, Model systems for photosynthesis act as photoinduced molecular wires in bilayers, *Electrochim. Acta.* 34 (1989) 1723.
- [20] P. Seta, E. Bienvenue, P. Maillard, Stacked zinc triporphyrin as a photoinduced molecular wire in bilayers, *Photochem. Photobiol.* 49 (1989) 537.
- [21] J.W. Arbogast, C.S. Foote, M. Kao, Electron transfer to triplet C₆₀, *J. Am. Chem. Soc.* 114 (1992) 2277.